Resonance splitting and broadening in axially deformed fermionic systems

E. S. Hernández and A. Kievsky
Departamento de Física, Facultad de Ciencias Exactas y Naturales, Universidad de Buenos Aires, 1428 Buenos Aires, Argentina
(Received 23 January 1986)

The dynamics of a tridimensional, axially degenerated vibration coupled to a finite Fermi system shaped as a cylindrical reservoir in the Markovian—plus—weak-coupling regime is investigated. The vibration is aimed at representing a normal mode of the fermion system and is extracted out of a hydrodynamical construction for the relative motion of a two-fluid mixture. Such a procedure provides a dispersion relation that has been proven to work properly in nuclear theory. A residual coupling between the mode and the heat reservoir constituted by the single-particle degrees of freedom is adopted and equations of irreversible evolution for the oscillator components and for the fermionic population can be obtained. This dynamical system is numerically integrated for a variety of container sizes and particle numbers and it is shown that thermodynamic magnitudes characterizing the attractor of the dynamical system, as well as typical relaxation times, can be consistently extracted from the numerical approach.

I. INTRODUCTION

The evidence of collective mode broadening in finite many-particle objects such as atoms, molecules, and nuclei provides an excellent example of an irreversible route to canonical equilibrium in systems far from the thermodynamic limit. In particular, an investigation of the origin and nature of resonances and their damping in finite Fermi systems such as nuclei is a challenging task, since up to now no complete, self-consistent treatment of resonant decay has been provided.[1–8] Approaches to the description of either the centroids or the widths of these collective degrees of freedom in nuclei and more general Fermi systems range from purely hydrodynamic[9] to purely microscopic[8] models, with a recent emphasis on the self-consistent buildup of broadened oscillations.[10–12] On the other hand, an attempt to extract half-lives out of a time evolution pattern of the vibration and the single-particle (SP) states in the heat bath has been recently provided.[1–7] In this approach, one essentially leaves aside the considerations regarding the structure of the mode on the grounds that the amount of violation of the Pauli principle can be proven to be small,[3] and solves the coupled dynamics of a quantal oscillator and the fermions in a heat reservoir. Calculations performed in extended[1,2,5–7] and finite Fermi systems such as spherical nuclei[3,4] cover a number of possibilities concerning the geometry of the reservoir and the nature—i.e., either elastic or inelastic—of the coupling to the vibration and in every situation already considered, a systematic approach to equilibration that accounts for finite half-lives is encountered.

In the present work we board a study of the dynamics of a tridimensional axially degenerated vibration coupled to a finite Fermi system shaped as a cylindrical container. This configuration is aimed at a model investigation, in future work, of resonance splitting and broadening in axially deformed nuclei and is conceived, at the present stage, rather as a problem in nonequilibrium statistical mechanics, since the selected interaction is mainly devised for didactical purposes and is not realistic enough to allow for experimental tests. It is an extension of the so-called quantal Brownian motion (QBM) model of collective mode damping to a peculiar geometry that makes room to straightforward introduction of a hydrodynamical construction yielding a dispersion relation and phonon wave functions. Equations of motion extracted in a standard fashion[1–7] are numerically integrated and several features of the approach to equilibrium of either oscillator or fermionic degrees of freedom can be analyzed, as well as the consistency of the asymptotic configuration on thermodynamic grounds.

In Sec. II, we describe the model and the perspectives that we have adopted in order to construct the free Hamiltonian and the interaction. In particular, we dedicate some space to describing the major characteristics of the above-mentioned construction, a well-founded one in nuclear theory,[9] that we find of interest due to the possibilities of applications to any Fermi system consisting of two distinct components, i.e., one charged and one neutral fluid. In Sec. III we briefly quote the QBM prescriptions for the time evolution of the mode and its heat bath. Section IV contains the description of the calculations and displays the results which are analyzed in Sec. V. The final summary is presented in Sec. VI.

II. THE MODEL

We are considering here a three-dimensional oscillator with axial symmetry immersed in a fermionic heat bath to which it couples through a particle-phonon interaction. The total Hamiltonian then reads

$$H = H_B + H_F + H_{BF} , \tag{2.1}$$

where B and F denote bosons and fermions, respectively.

We now perform a detailed discussion of each term appearing in Eq. (2.1).

A. The boson Hamiltonian

We assume that the heat bath consists of weakly interacting fermions located in a cylindrical reservoir with radius R and height L at a constant density n_0. This geometry has been selected as a crude first approximation to a finite deformed nucleus possessing the density of nuclear matter, namely $n_0=0.17$ particles/fm^3. If we write

$$H_F=H_F^{(0)}+V_F = \sum_A \varepsilon_A b_A^\dagger b_A + \tfrac{1}{4}\sum_{A,B,C,D} V_{ABCA}\, b_A^\dagger b_B^\dagger b_D b_C \quad (2.2)$$

the unperturbed SP energies ε_A are the eigenvalues of a cylindrical Schrödinger equation

$$-\frac{\hbar^2}{2m}\nabla^2\psi_A(r,\varphi,z)=\varepsilon_A\psi_A(r,\varphi,z) \quad (2.3)$$

satisfying the boundary condition on the surface $\psi_A(\text{surf})=0$. One finds

$$\psi_A(r,\varphi,z)=\psi_{nmn_z}(r,\varphi,z) =D_{nmn_z}J_m(k_m^n r)\cos(m\varphi)\sin(k_z z)\,, \quad (2.4)$$

where D_{nmn_z} is a normalization constant, $J_m(x)$ is a cylindrical Bessel function with wave number k_m^n such that $J_m(k_m^n R)=0$, m is an integer and the axial wave number is $k_z=\pi n_z/L$ for integer n_z. The SP energy then reads

$$\varepsilon_{mnn_z}=\frac{\hbar^2}{2m}\left[(k_m^n)^2+\frac{\pi^2}{L^2}n_z^2\right]. \quad (2.5)$$

The details of the two-body matrix elements V_{ABCD} are not relevant for the purpose of the present work.

B. The boson Hamiltonian

As mentioned above the boson Hamiltonian H_B describes a three-dimensional oscillator with cylindrical symmetry. In future applications to nuclear physics, such an oscillator will represent a collective oscillation of neutrons against protons giving rise to giant multiple resonances. Consequently, to the aim of establishing the frequencies of the vibration, we resort here to a quantized hydrodynamical model, which bears an old tradition in nuclear physics,[9] and can be utilized for any binary mixture with one charged and one neutral component where a charge oscillation starts. This is actually a two-fluid model whose total uniform density n_0 decomposes as

$$n_0=n_1(\mathbf{r},t)+n_2(\mathbf{r},t)\,, \quad (2.6)$$

where the labels 1 and 2 may denote protons and neutrons, respectively, or any other two subsystems of actual interest. Furthermore, the partial particle densities $n_i(\mathbf{r},t)$ are assumed to experience slight deviations from their equilibrium values n_1^0 and n_2^0 related by

$$\frac{n_1^0}{n_2^0}=\frac{N_1}{N_2} \quad (2.7)$$

with N_i the total number of type-i particles. In other words, if, for instance, n_1 varies as

$$n_1(\mathbf{r},t)=n_1^0[1+\eta(\mathbf{r},t)] \quad (2.8)$$

in order to fulfill both (2.6) and (2.7) we get

$$n_2(\mathbf{r},t)=n_2^0\left[1-\frac{N_1}{N_2}\eta(\mathbf{r},t)\right]. \quad (2.9)$$

In this model, one is mainly interested in the extraction of the compression modes associated with the relative motion of the fluid. This can be achieved if one imposes a variational principle upon a Lagrangian $L=T-U$ where (i) T is the relative kinetic energy,

$$T=\tfrac{1}{2}m\int n_r(\mathbf{r},t)v^2(\mathbf{r},t)d^3r \quad (2.10)$$

with n_r the reduced particle density

$$n_r=\frac{n_1 n_2}{n_0} \quad (2.11)$$

for particles of equal mass m and $\mathbf{v}$ the relative velocity of the fluids,

$$\mathbf{v}=\mathbf{v}_1-\mathbf{v}_2\,. \quad (2.12)$$

Notice that if the masses of the particles in type-1 and type-2 fluids are different, one should consider mass densities rather than particle densities in n_1 and n_2 (thus in n_0 and n_r). (ii) U is the potential energy for the particular problem one is describing. Since we are concerned with nuclear matter, the appropriate potential energy is the symmetry energy,

$$U\equiv E_{\text{sym}}=\frac{\mathcal{K}}{n_0}\int (n_1-n_2)^2 d^3r \quad (2.13)$$

with $\mathcal{K}$ a symmetry parameter given by a mass formula.[13] No electromagnetic force is taken into account in the nuclear matter approximation.

The normal modes of both relative velocity and reduced density are those modes of the Euler-Lagrange equations for the action $S=\int L\,dt$ subjected to the constraint $N=N_1+N_2=$constant. If the motion is irrotational, the velocity $\mathbf{v}$ is the gradient of a potential Φ and the Euler-Lagrange equations are just wave equations,

$$\nabla^2\psi=\frac{1}{u^2}\frac{\partial^2}{\partial t^2}\psi \quad (2.14)$$

for $\psi(\mathbf{r},t)=\eta(\mathbf{r},t)$ or $\Phi(\mathbf{r},t)$. The sound velocity u takes the form

$$u=\left[\frac{8\mathcal{K}}{m}\frac{N_1N_2}{(N_1+N_2)^2}\right]^{1/2} \quad (2.15)$$

in terms of the parameters of the model.

The cylindrical symmetry yields three normal modes, namely,

$$\psi_{nmn_z}^{(1)}=D_{nmn_z}^{(1)}J_m(q_m^n r)e^{im\varphi}\cos(q_z z)\,, \quad (2.16a)$$

$$\psi^{(2)}_{nmn_z}=D^{(2)}_{nmn_z}J_m(q^n_m r)e^{-im\varphi}\cos(q_z z)\ , \tag{2.16b}$$

$$\psi^{(3)}_{n0n_z}=D^{(3)}_{n0n_z}J_0(q^n_0 r)\cos(q_z z)\ , \tag{2.16c}$$

where m is an integer and the wave numbers q are provided by the zero-outflow boundary condition,

$$\hat{\mathbf{n}}\cdot\nabla\psi\,|_{\rm surf}=0\ . \tag{2.17}$$

One can then write the general solution of Eq. (2.14) as

$$\psi(\mathbf{r},t)=\sum_{\substack{n,n_z\\ m>0\\ i=1,2}}\alpha^{(i)}_{nmn_z}(t)\psi^{(i)}_{nmn_z}(\mathbf{r})+\sum_{n,n_z}\alpha^{(3)}_{n0n_z}(t)\psi^{(3)}_{n0n_z}(\mathbf{r})\ , \tag{2.18}$$

where the amplitudes $\alpha^{(i)}_{nmn_z}(t)$, $i=1,2,3$, are generalized coordinates. The coordinates for the velocity and density fields are related by the continuity equation that in the present situation takes the form

$$\frac{\partial\eta}{\partial t}-\frac{n_2(0)}{n_0}\nabla^2\varphi=0\ . \tag{2.19}$$

Now, with the help of the general solutions (2.18), the procedure to extract the quantized vibrations of the two-fluid system is as follows. First, one considers the Lagrangian $L=T-U$ corresponding to Eqs. (2.10) and (2.13); the orthonormality of the normal modes (2.16) yields then a quadratic expression in terms of the generalized coordinates $\alpha^{(i)}_{nmn_z}$ and their derivatives $\dot{\alpha}^{(i)}_{nmn_z}$. Since the relation (2.19) holds, only the coordinates describing the excess density $\eta(\mathbf{r},t)$ appear in the Lagrangian. Secondly, one extracts the generalized momenta,

$$\Pi^{(i)}_{nmn_z}=\frac{\partial L}{\partial\dot{\alpha}^{(i)}_{nmn_z}}\ , \tag{2.20}$$

and writes down a Hamiltonian,

$$H=\sum_{i,n,m,n_z}\dot{\alpha}^{(i)}_{nmn_z}\Pi^{(i)}_{nmn_z}-L\ . \tag{2.21}$$

This Hamiltonian can be straightforwardly quantized when one has introduced canonical commutation relations between the generalized coordinates and their respective momenta. Thus, the final step in this procedure is to construct the boson operators,

$$\Gamma^{\dagger(i)}_{nmn_z}=\frac{1}{2}\left[\left[\frac{2B^{(i)}_{nmn_z}\omega^{(i)}_{nmn_z}}{\hbar}\right]^{1/2}\alpha^{(i)}_{nmn_z}-i\left[\frac{2}{\hbar B^{(i)}_{mnn_z}\omega^{(i)}_{mnn_z}}\right]^{1/2}(-1)^m\Pi_{n,-mn_z}\right]\ , \tag{2.22}$$

where $B^{(i)}_{nmn_z}$ and $\omega^{(i)}_{nmn_z}$ are, respectively, the inertia and frequency parameters that explicitly show up in the first step.[9] These quantities are degenerated on the polar plane and are known functions of the model parameters as displayed in Ref. 9. Accordingly, the noninteracting boson Hamiltonian reads

$$H=\sum_{\substack{n,n_z\\ m>0}}\hbar\omega_{nmn_z}(\Gamma^\dagger_{nmn_z}\Gamma_{nmn_z}+\Gamma^\dagger_{n,-mn_z}\Gamma_{n,-mn_z}+1)+\sum_{n,n_z}\hbar\omega_{n0n_z}(\Gamma^\dagger_{n0n_z}\Gamma_{n0n_z}+\tfrac{1}{2}) \tag{2.23}$$

with frequencies

$$\omega_{nmn_z}=uq_{nmn_z}=u[(q^n_m)^2+q^2_{n_z}]^{1/2}\ . \tag{2.24}$$

We drop the superscript (i) in the frequencies and in the phonon operators, since the polar degeneracy for $i=1,2$ allows us to identify two different ones according to m being different or equal to zero ($i=3$ in the latter case).

The model Hamiltonian in Eq. (2.1) contains just three modes of Hamiltonian (2.23), actually those able to build up a three-dimensional oscillator with axial symmetry. These are the components of the lowest dipole mode $n=1$, $m=-1,0,1$, and $n_z=0$; we select then a boson Hamiltonian H_B as

$$H_B=\hbar\omega_{110}(\Gamma^\dagger_{110}\Gamma_{110}+\Gamma^\dagger_{1,-10}\Gamma_{1,-10}+1)+\hbar\omega_{100}(\Gamma^\dagger_{100}\Gamma_{100}+\tfrac{1}{2})\ . \tag{2.25}$$

This choice means that in the current model one implicitly assumes that higher multipoles are unimportant, either because they lie too high in energy for the adopted geometry or because they do not couple to the fermionic excitations in order to participate in the dynamics to a relevant extent.

Note that the phonon operators in Eq. (2.25) possess well-defined angular momentum projection; indeed, one has

$$L_z\Gamma^\dagger_{1,\pm m0}\,|\,0\rangle=\pm\hbar m\,\Gamma^\dagger_{1,\pm m0}\,|\,0\rangle\ . \tag{2.26}$$

The frequencies can be calculated from Eq. (2.24) and read

$$\omega_{1m0}=uq_{1m0}\equiv uq^1_m \tag{2.27}$$

since $q_{n_z}=\pi n_z/L=0$. The momenta q^1_m are the roots of the equations

$$J_1(q^1_1R)-q^1_1RJ_0(q^1_1R)=0\ , \tag{2.28a}$$

$$J_1(q^1_0R)=0\ . \tag{2.28b}$$

One finds

$$q^1_1=\frac{1.841}{R},\quad q^1_0=\frac{3.832}{R}\ . \tag{2.29}$$

C. The interaction Hamiltonian

The coupling between bosonic and fermionic degrees of freedom is a standard particle-phonon interaction in the present model. It reads

$$H_{BF}=\sum_{i=1}^{3}\sum_{\alpha,\mu}\lambda^{(i)}_{\alpha\mu}\Gamma^{\dagger(i)}b^\dagger_\mu b_\alpha+\text{H.c.}\ , \tag{2.30}$$

where the matrix element $\lambda_{\alpha\mu}^{(i)}$ is assumed to represent the scalar product,

$$\lambda_{\alpha\mu}^{(i)}=\int d^3r_p \int d^3r_{\rm ph}\,\psi_\mu^*(\mathbf{r}_p)\psi^{*(i)}(\mathbf{r}_{\rm ph}) \times V(\mathbf{r}_p,\mathbf{r}_{\rm ph}^{(i)})\psi_\alpha(\mathbf{r}_p)\ . \tag{2.31}$$

In this expression, $\mathbf{r}_p$ and $\mathbf{r}_{\rm ph}$ denote particle and phonon coordinates, respectively; $V(\mathbf{r}_p,\mathbf{r}_{\rm ph}^{(i)})$ is a model interaction between a fermion at $\mathbf{r}_p$ and a type-i phonon at $r_{\rm ph}^{(i)}$ and ψ denotes either wave function. We further adopt the potential

$$V(\mathbf{r}_p,\mathbf{r}_{\rm ph}^{(i)})=\lambda\delta(\mathbf{r}_p-\mathbf{r}_{\rm ph})\ \text{ all } i \tag{2.32}$$

thus

$$\lambda_{\alpha\mu}^{(i)}=\lambda\int d^3r\,\psi_\mu^*(\mathbf{r})\psi_{\rm ph}^{(i)*}(\mathbf{r})\psi_\alpha(\mathbf{r})\ . \tag{2.33}$$

The SP wave functions are those in Eq. (2.4); as for the free-phonon wave functions we adopt the cylindrical normal modes whose shape is displayed in Eqs. (2.16).

Expression (2.33) factorizes as three integrals; the radial one can be evaluated with the help of standard tables. We just quote the result here that exhibits the current selection rule as

$$\lambda_{\alpha\mu}^{(1)}=\lambda_{\alpha\mu}^{(2)} =\lambda\delta_{n_{z_\alpha},n_{z_\mu}}\begin{cases}F(k_\alpha,k_\mu,q_{110},1)\delta_{m_\alpha,a}\delta_{m_\mu,0}\\ F(k_\mu,k_\alpha,q_{110},1)\delta_{m_\alpha,0}\delta_{m_\mu,1}\ ,\end{cases} \tag{2.34a}$$

$$\lambda_{\alpha\mu}^{(\ )}=\lambda\delta_{n_{z_\alpha},n_{z_\mu}}\delta_{m_\alpha,m_\mu}F(k_\alpha,q_{100},k_\mu,m_\alpha)\,, \tag{2.34b}$$

with the kernel

$$F(k_1,k_2,k_3,m)=\begin{cases}\dfrac{1}{\pi k_1k_3}\dfrac{\cos(m\mathscr{A})}{\sin\mathscr{A}}+O((kR)^1)\ \text{ if }\ |k_1-k_2|<k_3<k_1+k_2\\ 0\ \text{ if } k_3<|k_1-k_2|\ \text{ or }\ k_3>k_1+k_2\ ,\end{cases} \tag{2.34c}$$

the argument $\mathscr{A}$ being

$$\mathscr{A}=\cos^{-1}\left[\frac{k_1^2+k_3^2-k_2^2}{2k_1k_3}\right]. \tag{2.34d}$$

The kernel in Eq. (2.34c) vanishes unless a triangular relationship among momenta is fulfilled. This condition reflects a restricted linear-momentum conservation; of course, strict conservation is meaningless in the present case since the geometry does not allow the components of the linear momentum to be good quantum numbers.

III. THE DYNAMICS

We are concerned here with the time evolution of the reduced density operators representing either the bosonic or the heat-bath degrees of freedom, ρ_B and ρ_F, respectively. A standard reduction procedure on the Liouville–von Neumann equation of motion[1–7] combined with a Markovian-like hypothesis yields a pair of coupled equations of irreversible evolution. The details of the approach have been extensively discussed in prior works[1–7,14] and we will not repeat them here. The general scheme is as follows; we express the density operators as

$$\rho_B=\prod_{i=1}^{3}\rho_B^{(i)}\ , \tag{3.1a}$$

$$\rho_B^{(i)}=\sum_{nn'}\rho_{nn'}^{(i)}\,|\,n\,\rangle\langle\,n'\,|\ ,\quad i=1,2,3 \tag{3.1b}$$

with $|\,n\,\rangle$ an oscillator (Fock) basis, and

$$\rho_F=\frac{1}{N!}\det(\rho_1)+\rho_F^{(c)} \tag{3.2}$$

with $\det(\rho_1)$ denoting a Slater determinant of SP densities ρ_1 whose spectral decomposition reads

$$\rho_1=\sum_{AA'}\rho_{AA'}\,|\,A\,\rangle\langle\,A'\,| \tag{3.3}$$

on the SP basis of Eq. (2.4), and $\rho_F^{(c)}$ is a correlation contribution induced by the two-body interaction. The reduction procedure in the Markovian–plus–weak-coupling regime yields equations of motion that, once the off-diagonal matrix elements in Eqs. (3.1b) and (3.3) have decayed[15]—i.e., very close to equilibration—adopt the form

$$\dot\rho_0^{(i)}=W_+^{(i)}\rho_1^{(i)}-W_-^{(i)}\rho_0^{(i)}\ , \tag{3.4a}$$

$$\dot\rho_n^{(i)}=W_+^{(i)}(\rho_{n+1}^{(i)}-\rho_n^{(i)})+W_-^{(i)}(\rho_{n-1}^{(i)}-\rho_n^{(i)})\ , \tag{3.4b}$$

$$\dot\rho_N^{(i)}=-W_+^{(i)}\rho_N^{(i)}+W_-^{(i)}\rho_{N-1}^{(i)} \tag{3.4c}$$

for the boson occupation probabilities, and

$$\dot{\rho}_A = \sum_{i=1}^{3} \sum_{\alpha,\mu} |\lambda_{\alpha\mu}^{(i)}|^2 \mathcal{F}(\omega^i - \omega_{\alpha\mu}) \{ \delta_{A\mu} [(1-\rho_0^{(i)})\rho_\mu (1-\rho_\alpha) - (1-\rho_N^{(i)})\rho_\alpha (1-\rho_\mu)] + \delta_{A\alpha} [(1-\rho_N^{(i)})\rho_\alpha (1-\rho_\mu) - (1-\rho_0^{(i)})\rho_\mu (1-\rho_\alpha)] \} + \dot{\rho}_{\text{kin}} \quad (3.4d)$$

for the fermion occupation numbers.

As in previous works[1-7,14] the quantities $W_{\pm}^{(i)}$ are transition rates whose expression is

$$W_{\pm}^{(i)} = \sum_{\alpha\mu} |\lambda_{\alpha\mu}^{(i)}|^2 \mathcal{F}(\omega^{(i)} - \omega_{\alpha\mu}) \rho_\mu (1-\rho_\alpha) \; . \quad (3.5)$$

Both in Eq. (3.4d) and in Eq. (3.5) the symbol $\mathcal{F}(\omega^{(i)} - \omega_{\alpha\mu})$ denotes a Lorentzian filter,[2-4,6]

$$\mathcal{F}(\omega^{(i)} - \omega_{\alpha\mu}, \gamma) = \frac{\gamma}{\hbar(\omega^{(i)} - \omega_{\alpha\mu})^2 + \hbar\gamma^2} \quad (3.6)$$

that accounts for energy nonconservation, since in order to derive Eq. (3.4) one has assumed that the particle-phonon interaction lasts a finite lapse $\tau_c = \gamma^{-1}$. The quantity $\hbar\gamma$ is then an energy spread occurring at scattering and should be much larger than any typical energy parameter in the total system, if the Markovian approximation holds. Furthermore, the kinetic time derivative $\dot{\rho}_{\text{kin}}$ in Eq. (3.4d) is the Boltzmann-like collision rate induced by the two-body interaction in (2.2); since we are interested in examining the role of the particle-phonon coupling, we will disregard this contribution in what follows.

IV. DESCRIPTION OF THE CALCULATIONS

We have numerically integrated the dynamical system (3.4) for different particle numbers N and different dimensions R and L. The latter have been chosen in order to reproduce (i) together with N, a typical nuclear matter density of $n_0 = 0.17$ fermions per unit volume and (ii) a ratio R/L consistent with an average nuclear quadrupole deformation. In every case the boson frequencies have been evaluated according to Eqs. (2.27) and (2.29). The SP spectrum has been built up with Eq. (2.5), allowing for a fourfold spin-isospin degeneracy. All those SP states above the Fermi level that participate in the dynamics up to a two-step phonon generation have been included. This criterion for spectrum truncation was adopted after several trials once it was established that the calculation turned out to be stable and saturated if further extension of the SP spectrum was allowed.

Typical results are displayed in Table I. The columns are labeled by the number of particles and each of them contains, in addition to the parameters R, L, the Fermi energy ε_F, and the energies $\hbar\omega_{110}, \hbar\omega_{100}$ (in units of $\hbar^2/2m$), the energies of the fermionic and the bosonic systems evaluated at $t=0$ and these energies, as well as the corresponding entropies, extrapolated from our numerical treatment for t increasing up to infinity. Indeed, such an extrapolation is rather trivial since our long-time runs exhibit overall equilibration of the subsystems under consideration. This fact can be appreciated in Fig. 1, where the entropies of these three sets of degrees of freedom are displayed as a function of time for $N=52$.

The results shown in Table I and Fig. 1 correspond to an initial configuration with the circular phonons ($m=\pm 1$) excited, the axial phonon ($m=0$) at its ground state, and a cold Fermi gas. The evolution of the SP distribution for $N=100$ particles can be observed in Fig. 2. For future analysis, we show as well in Figs. 3 and 4 the corresponding evolution for the initial conditions (i) one axial phonon excited, the circular ones deexcited and (ii) the three phonons excited, respectively. The SP states $|nmn_z\rangle$ and their energies are given in Table II.

All these computations have been performed for an inelasticity spread $\hbar\gamma = 0.5$ (in the current energy units). It was chosen so as to broaden each SP state level to the extent to which it overlaps 2–4 neighboring states. We remind the reader that the value of this parameter is irrelevant at the present state of the calculations. It plays the role of a representative of disregarded open channels capable of driving flux out of a colliding particle-phonon system and convert the discrete SP spectrum into a continuous one, without which a dissipative dynamics could not take place.[16]

V. ANALYSIS OF THE RESULTS

The first observation from inspection of Fig. 1 is the overall equilibration attained by the three subsystems and their different time scales. Notice that the overshooting displayed by the entropy of the degenerate oscillator and its subsequent decrease to a saturation figure is not in contradiction with the second law of thermodynamics since the total entropy is an increasing magnitude.

TABLE I. The initial energies and the asymptotic energies and entropies of the three subsystems under study for different numbers of fermions in the reservoir with radius R and height L. The Fermi energy for each selection of dimensions is indicated as well as the two phonon energies.

N	20	52	100	200
R	2.38	3.5	4.5	5.57
L	3.17	4.68	6.0	7.5
ε_F	2.84	2.60	2.44	2.48
$\hbar\omega_{110}$	1.53	1.04	0.81	0.65
$\hbar\omega_{100}$	3.18	2.16	1.68	1.36
$E_F(0)$	36.9	80.2	128.1	275.2
$E_{B_1}(0)$	1.53	1.04	0.81	0.65
$E_{B_2}(0)$	0.00	0.00	0.00	0.00
$E_F(\infty)$	45.0	84.9	131.5	277.9
$E_{B_1}(\infty)$	0.177	0.047	0.03	0.013
$E_{B_2}(\infty)$	0.013	0.04	0.002	0.001
$S_F(\infty)/N$	0.750	0.379	0.21	0.120
$S_{B_1}(\infty)$	0.373	0.188	0.16	0.100
$S_{B_2}(\infty)$	0.026	0.014	0.01	0.003

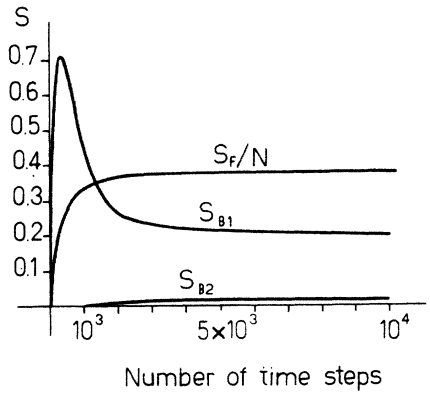

FIG. 1. The time evolution of the entropy of the bosonic and the fermionic systems (in arbitrary units).

From the data displayed in Table I one can extract several interesting quantities. As a matter of fact, one might be interested in testing the adequacy of a statistical description for systems far from the thermodynamic limit. This can be achieved in various ways and we have chosen the following: if we assume that the vibrations reach equilibrium at a heat-bath temperature T, the energy would read, for any of them,

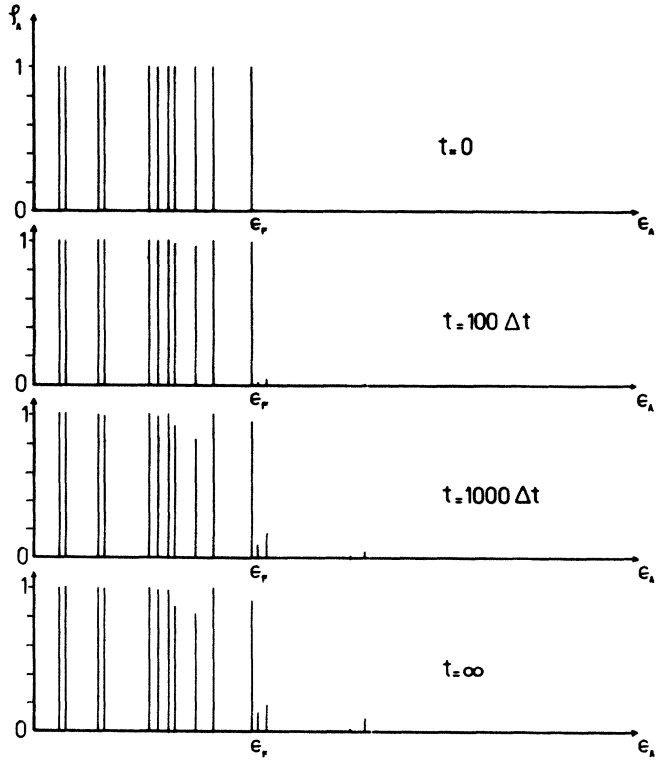

FIG. 2. The distribution of the fermions at different time steps during the evolution. The initial conditions correspond to an excited circular vibration and an axial component at its ground state.

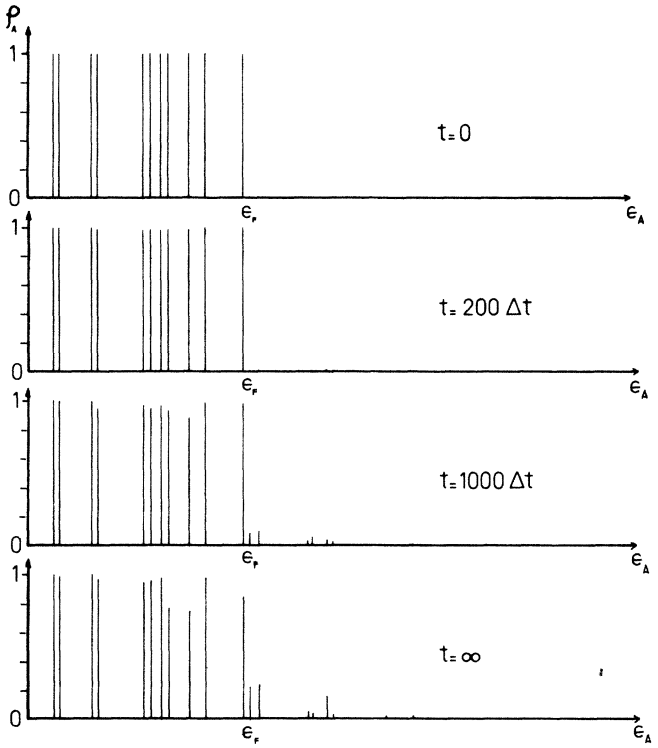

FIG. 3. Same as in Fig. 2 with one axial phonon excited and the circularly degenerated oscillator at its ground state.

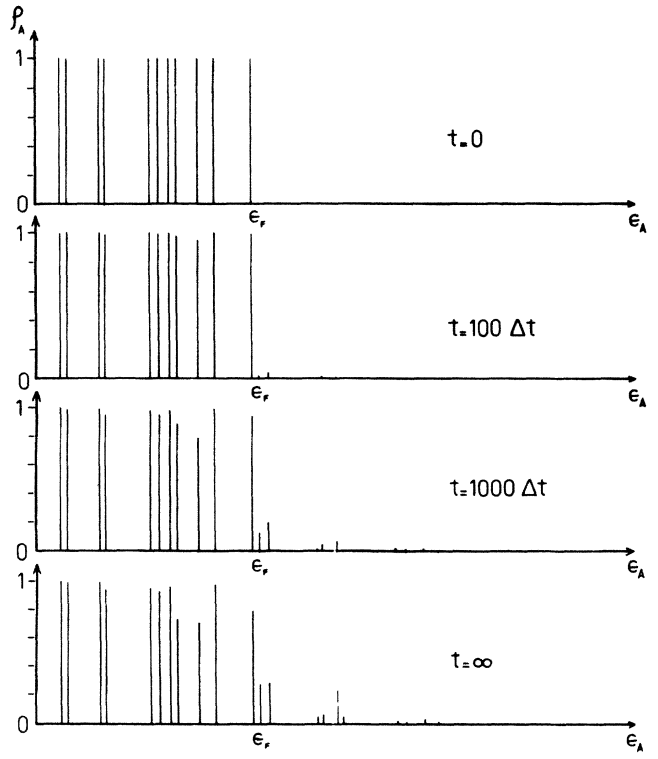

FIG. 4. Same as in Figs. 2 and 3 with the three normal modes initially excited.

TABLE II. The fermion orbitals and energies for $N=100$ particles in the container with the dimensions indicated in Table I. Only those orbitals are displayed that effectively participate in collision events with a vibrational mode in the current model.

nmn_z	ε_{nmn_z}
100	0.28
101	0.35
110	0.72
111	0.79
120	1.30
104	1.38
200	1.50
201	1.57
114	1.81
130	2.01
210	2.43
211	2.50
204	2.60
220	3.50
214	3.53
300	3.70
301	3.77
230	4.70
304	4.79
310	5.11
311	5.18
314	6.21

$$U_B=\frac{\hbar\Omega}{e^{\hbar\Omega/T}-1}\ . \tag{5.1}$$

Consequently, we can extract a temperature T out of (5.1) for each $E_{Bi}(\infty)$ in Table I. Furthermore, we can evaluate the theoretical canonical entropy of each oscillator as

$$S_B(T)=\frac{U_B}{T}-\ln(1-e^{-\Omega/T})\ . \tag{5.2}$$

These temperatures and entropies are shown in Table III for the same column labeling as in Table I. We can appreciate (i) the excellent agreement between the two temperatures T_{Bi} at each column; (ii) the excellent agreement between the canonical entropies evaluated according to (5.2) for each mode and the corresponding saturation entropies $S_{Bi}(\infty)$ obtained out of the time evolution (cf. Table I); and (iii) these excellent agreements in (i) and (ii) improve, in relative figures, as N increases. It is worth pointing out that these figures are rather more than acceptable even in the case of a low particle number such as 20.

In order to complete the undergoing argument, we have computed the energy and chemical potential of an extended, degenerate Fermi gas,

$$U_F(T)=U_F(0)\left[1+\frac{5\pi^2}{12}\left[\frac{T}{T_F}\right]^2\right]\ , \tag{5.3a}$$

$$\mu(T)=\varepsilon_F\left[1-\frac{\pi^2}{12}\left[\frac{T}{T_F}\right]^2\right]\ , \tag{5.3b}$$

for a temperature $\tilde{T}=(T_{B_1}+T_{B_2})/2$ at each column of Table I. In addition, we have chosen to express the chemical potential in terms of energy and entropy as

$$\mu'(T)=(\tfrac{5}{3}U_F-S_FT)/N \tag{5.4}$$

and evaluated this quantity for $T=\tilde{T}$ introducing the values for $U_F(\infty)$ and $S_F(\infty)$. This computation was selected rather than the evaluation of $S_F(T)$ out of $U_F(T)$ and $\mu_F(T)$ in order to eliminate instabilities due to numerical rounding-off. The results are also shown in Table III. A due comparison makes evident that (i) the canonical energy $U_F(T)$ lies within a fringe narrower than a rough 2%, even for a low particle number such as 20, and (ii) for $N\geqq 52$ the chemical potentials computed according to the choices (5.3b) and (5.4) are in excellent agreement, demonstrating the thermodynamic consistency of the evolution data.

Different initial conditions make room for the behavior of the fermionic system drawn in Figs. 2–4. Before entering a detailed analysis of these figures we wish to quote that from our evolution data we can extract identical conclusions to those already mentioned in connection with Tables I and III plus the following features: (i) according to different initial excitations—in other words, different amounts of available phonon energy to share among the participating degrees of freedom—various temperatures, thermal energies, and entropies show up that increase with the total initial excitation energy; (ii) the chemical potential evaluated with Eq. (5.3b) is $\mu_F(\tilde{T})=2.40$ and that corresponding to Eq. (5.4) is $\mu'_F=2.14$, in each case they are constant figures independent of the initial conditions as well as of the final equilibrium temperatures corresponding to a truly degenerate Fermi gas.

Now, Figs. 2–4 possess the following characteristics.

TABLE III. The heat-bath temperatures evaluated according to Eq. (5.1) for either oscillator; the corresponding entropies; the internal energy of a free Fermi gas at the average temperature $\tilde{T}=(T_{B_1}+T_{B_2})/2$; the chemical potential of the referred Fermi gas and that calculated with Eq. (5.4); the characteristic times (5.5) for the three subsystems. These data are displayed for the same column specifications as in Table I.

T_{B_1}	0.675	0.332	0.242	0.166
T_{B_2}	0.578	0.343	0.249	0.170
$S_{B_1}(T_{B_1})$	0.372	0.186	0.160	0.100
$S_{B_2}(T_{B_2})$	0.026	0.013	0.009	0.003
$U_F(\tilde{T})$	44.4	85.7	133.4	280.4
$\mu(\tilde{T})$	2.73	2.56	2.40	2.47
$\mu'(\tilde{T})$	3.28	2.59	2.14	2.30
$\tau(E_{B_1})$	$1900\Delta t$	$850\Delta t$	$620\Delta t$	$600\Delta t$
$\tau(E_{B_2})$	$1400\Delta t$	$500\Delta t$	$310\Delta t$	$310\Delta t$
$\tau(E_F)$	$2800\Delta t$	$900\Delta t$	$700\Delta t$	$700\Delta t$

In all cases the levels suffering the largest occupation change are those that lie in the neighborhood of the Fermi level and that participate in direct coupling to the circularly degenerate—i.e., $m=\pm 1$—phonons. These are the SP states $|nmn_z\rangle = |201\rangle$, $|114\rangle$, and $|210\rangle$ above the Fermi level and their respective partners below this state, actually the orbitals $|211\rangle$, $|204\rangle$, and $|300\rangle$. Each of these states may in turn couple to the $m=0$ phonon through a different partner. Other orbitals suffer less significant variations in their occupation numbers, although a careful comparison of the pictures in Figs. 2–4 shows that the more significant changes at those states take place when the type-3 phonon ($m=0$) is initially excited. The reason for this behavior is that in such a case, both the selection rules involved in the particle–axial-phonon coupling and the larger amount of available excitation energy provide important time derivatives for the SP occupation numbers of those states at short times. One could additionally notice (cf. Figs. 3 and 4) that the larger the initial excitation energy, the larger is the variation in the population of originally occupied or unoccupied SP states.

In this respect, it can be observed as well that the relaxation of the Fermi distribution depends on the initial conditions. Even more, the rates of equilibration for the three subsystems under consideration depend on the dimensions and particle number. Table III displays a set of relaxation times τ for these subsystems defined as

$$E(\tau)=E(\infty)+\frac{E(0)-E(\infty)}{e} . \tag{5.5}$$

This table shows (a) the Fermi system takes longer than either boson system to reach equilibrium; (b) the degenerate oscillator presents a characteristic relaxation time slightly smaller than the Fermi gas, but about a factor of 2 higher than the $m=0$ vibration, provided that the latter is initially at its ground state; and (c) in case this axial oscillator is excited at $t=0$, it drives the circular one to equilibrium at a higher rate and the relationship quoted in (b) is reversed. Such an inversion of the time figures occurs because the more important collision events involve SP states close to the Fermi surface, able to couple to $m=\pm 1$ phonons. Other transitions—that may involve the same orbitals coupled to the $m=0$ phonon—appear as largely inhibited by the energy conservation filter. This brings as a consequence that if such a phonon is initially excited, its decay suffers a relative delay since it may not evolve until the fermion population has undergone, via its coupling to the circular vibration, a change that allows the participation of blocked—i.e., not near to the Fermi surface—SP orbitals.

As a final remark, we must point out that the total energy is not strictly conserved. This is not surprising in view of the inelastic collisions considered here. However, the energy loss is always kept at a low percent and should not be considered an important figure of this calculation.

VI. SUMMARY

In this work we have designed a model that intends to simulate in a very low-order approximation the expected dynamics when a three-dimensional, circularly degenerated harmonic vibration in a fermion fluid excites and decays via its coupling to the excitons. In order to carry out this low-order approximation, we have disregarded any attempt to describe the motion in a self-consistent fashion and considered two distinct systems, actually a boson and a fermion field and a mutual coupling. The origin of the former is traced back to a two-fluid model that, although devised to describe giant resonances in nuclei, may also be well-suited to feature charge oscillations in binary mixtures. Once the normal modes of the relative motion of the fluids are extracted in a cylindrical geometry with rigid walls, the dipole contribution to the quantized Hamiltonian is adopted as the boson Hamiltonian of the model, assumed to couple to a generic fermion gas in a cylinder. In this way one has extracted a convenient dispersion relation which has already proven to be rather adequate for nuclear purposes.[9]

Equations of irreversible evolution of both the boson and the fermion degrees of freedom are extracted in the frame of the QBM model and numerically solved for various selections of container sizes, particle numbers, and initial conditions. Although all quantities are expressed in arbitrary units, they bear the relationships that are appropriate for nuclear scales. The analysis of the results makes evident a number of features, as follows. First, one realizes that the model provides a proper oscillator-bath thermodynamics for sufficiently long times, even for low particle numbers. In fact, one can demonstrate that consistent thermal variables and state functions such as temperature, energy, entropy, and chemical potential can be extracted. Secondly, the time evolution of the Fermi sea can be photographed at several steps and the population dynamics can be clearly interpreted on microscopic grounds. Finally, figures for characteristic relaxation times can be provided and their relative sizes can be traced to the initial configuration and its subsequent disarrangement.

It remains to be proven whether this oversimplified cylindrical geometry is a reasonable order-of-magnitude approximation to a realistic situation taking place in a spheroidal reservoir such as a nucleus. A numerical solution of the wave equation or employment of harmonic spheroidal functions[17] is then demanded. Calculations along this line are in progress and will be presented elsewhere.

ACKNOWLEDGMENTS

The authors are indebted to the Consejo Nacional de Investigaciones Científicas y Técnicas (CONICET) of Argentina for financial support and to the Programa de Investigaciones en Física del Plasma at their home institution for generous access to their computing facilities. We are grateful to Dr. H. Cataldo for many useful discussions and critical reading of this manuscript. This work was partially supported by Grants No. 9413d/85 from CONICET and No. 11473/84 from Secretaría de Ciencia y Técnica of Argentina.

[1]E. S. Hernández and C. O. Dorso, Phys. Rev. C **29**, 1510 (1984).
[2]C. O. Dorso and E. S. Hernández, Phys. Rev. C **29**, 1523 (1984).
[3]E. S. Hernández and C. O. Dorso, Phys. Rev. C **30**, 1711 (1984).
[4]V. de la Mota, C. O. Dorso, and E. S. Hernández, Phys. Lett. **143B**, 279 (1984).
[5]E. S. Hernández and A. Kievsky, Phys. Rev. A **32**, 1810 (1985).
[6]A. Kievsky and E. S. Hernández, Physica A (to be published).
[7]H. M. Cataldo, E. S. Hernández, and C. O. Dorso Physica A (to be published).
[8]G. Bertsch, Rev. Mod. Phys. **55**, 287 (1983).
[9]J. M. Eisenberg and W. Greiner, *Nuclear Theory* (North-Holland, Amsterdam, 1972), Vol. 1.
[10]C. Yannouleas, Phys. Lett. **157B**, 129 (1985).
[11]M. C. Nemes and A. F. R. de Toledo Piza, Z. Phys. A **310**, 339 (1983).
[12]S. Ayik and M. Dworzecka, Phys. Rev. Lett. **54**, 534 (1985).
[13]W. D. Myers and W. J. Swiatecki, Ann. Phys. (N.Y.) **55**, 395 (1969).
[14]E. S. Hernández, Physica **132A**, 28 (1985).
[15]C. O. Dorso and E. S. Hernández, Phys. Rev. C **26**, 528 (1982).
[16]C. George, I. Prigogine, and L. Rosenfeld, K. Dan. Vidensk. Selsk. Mat.-Fys. Medd. **38**, No. 12 (1972).
[17]*Handbook of Mathematical Functions*, edited by M. Abramowitz and I. Stegun (Dover, New York, 1972).